

Flagellar Localization of a *Helicobacter pylori* Autotransporter Protein

Jana N. Radin,^a Jennifer A. Gaddy,^a Christian González-Rivera,^b John T. Loh,^a Holly M. Scott Algood,^{a,c} Timothy L. Cover^{a,b,c}

Department of Medicine, Vanderbilt University, School of Medicine, Nashville, Tennessee, USA^a; Department of Pathology, Microbiology and Immunology, Vanderbilt University, School of Medicine, Nashville, Tennessee, USA^b; Veterans Affairs Tennessee Valley Healthcare System, Nashville, Tennessee, USA^c

J.N.R. and J.A.G. contributed equally to this work.

ABSTRACT *Helicobacter pylori* contains four genes that are predicted to encode proteins secreted by the autotransporter (type V) pathway. One of these, the pore-forming toxin VacA, has been studied in great detail, but thus far there has been very little investigation of three VacA-like proteins. We show here that all three VacA-like proteins are >250 kDa in mass and localized on the surface of *H. pylori*. The expression of the three *vacA*-like genes is upregulated during *H. pylori* colonization of the mouse stomach compared to *H. pylori* growth *in vitro*, and a wild-type *H. pylori* strain outcompeted each of the three corresponding isogenic mutant strains in its ability to colonize the mouse stomach. One of the VacA-like proteins localizes to a sheath that overlies the flagellar filament and bulb, and therefore, we designate it FaaA (flagella-associated autotransporter A). In comparison to a wild-type *H. pylori* strain, an isogenic *faaA* mutant strain exhibits decreased motility, decreased flagellar stability, and an increased proportion of flagella in a nonpolar site. The flagellar localization of FaaA differs markedly from the localization of other known autotransporters, and the current results reveal an important role of FaaA in flagellar localization and motility.

IMPORTANCE The pathogenesis of most bacterial infections is dependent on the actions of secreted proteins, and proteins secreted by the autotransporter pathway constitute the largest family of secreted proteins in pathogenic Gram-negative bacteria. In this study, we analyzed three autotransporter proteins (VacA-like proteins) produced by *Helicobacter pylori*, a Gram-negative bacterium that colonizes the human stomach and contributes to the pathogenesis of gastric cancer and peptic ulcer disease. We demonstrate that these three proteins each enhance the capacity of *H. pylori* to colonize the stomach. Unexpectedly, one of these proteins (FaaA) is localized to a sheath that overlies *H. pylori* flagella. The absence of FaaA results in decreased *H. pylori* motility as well as a reduction in flagellar stability and a change in flagellar localization. The atypical localization of FaaA reflects a specialized function of this autotransporter designed to optimize *H. pylori* colonization of the gastric niche.

Received 20 December 2012 Accepted 11 March 2013 Published 9 April 2013

Citation Radin JN, Gaddy JA, González-Rivera C, Loh JT, Scott Algood HM, and Cover TL. 2013. Flagellar localization of a *Helicobacter pylori* autotransporter protein. mBio 4(2): e00613-12. doi:10.1128/mBio.00613-12.

Editor Rino Rappuoli, Novartis Vaccines and Diagnostics

Copyright © 2013 Radin et al. This is an open-access article distributed under the terms of the [Creative Commons Attribution-NonCommercial-ShareAlike 3.0 Unported license](https://creativecommons.org/licenses/by-nc-sa/3.0/), which permits unrestricted noncommercial use, distribution, and reproduction in any medium, provided the original author and source are credited.

Address correspondence to Timothy L. Cover, timothy.l.cover@vanderbilt.edu.

Helicobacter pylori is a Gram-negative bacterium that colonizes the stomach in about 50% of humans worldwide (1–4). *H. pylori* colonization of the stomach results in gastric mucosal inflammation and is a significant risk factor for the development of distal gastric adenocarcinoma and peptic ulcer disease (3–5). One of the major virulence factors of *H. pylori* is a secreted protein known as vacuolating toxin (VacA) (7–9, 12). VacA is produced as a 140-kDa VacA protoxin that undergoes proteolytic cleavage to yield an 88-kDa protein that exhibits toxin activity (10, 11). The 88-kDa protein is secreted as a soluble protein into the extracellular space, or alternatively, it can remain attached to the bacterial cell surface (12, 13). VacA inserts into membranes to form anion-selective channels and can cause a wide array of alterations in host cells (7–9, 12).

Analysis of *H. pylori* genomes has revealed the existence of three *vacA*-like genes (14, 15). In strains 26695 and J99 (the first two *H. pylori* strains for which complete genome sequences were determined), these are designated HP0289/JHP0274, HP0609-0610/JHP0556, and HP0922/JHP0856 (14, 15). Several large-scale transposon mutagenesis studies provided evidence that two of the

vacA-like genes are important for colonization of the rodent stomach by *H. pylori*. Specifically, a signature-tagged mutagenesis screen identified HP0289/JHP0274 as a gene required for *H. pylori* colonization of the gerbil stomach (16). HP0289/JHP0274 was required for colonization of the mouse stomach by *H. pylori* strain LSH100 (a derivative of G27) but not by *H. pylori* strain SS1 (17). Another transposon mutagenesis screen identified HP0609/JHP0556 as a gene required for *H. pylori* colonization of the mouse stomach (18). The HP0289/JHP0274 promoter is upregulated upon *H. pylori* colonization of the mouse stomach compared to *H. pylori* growth *in vitro* (6), and a recent study showed that, in comparison to a wild-type *H. pylori* strain, an HP0289/JHP0274 mutant stimulated greater expression of interleukin 8 (IL-8) and tumor necrosis factor alpha (TNF- α) by gastric epithelial cells; therefore, it was proposed that the protein encoded by HP0289/JHP0274 (also known as ImaA) has immunomodulatory properties (17).

The genes encoding the VacA-like proteins are among the largest in the *H. pylori* genome and encode proteins with predicted molecular masses of 313 kDa, 348 kDa, and 260 kDa (correspond-

ing to the genes JHP0274, JHP0556, and JHP0856, respectively, in strain J99 (14, 15). Comparison of the sequences of the three VacA-like proteins with that of VacA shows that the highest level of similarity is within the C-terminal domains; other regions of the proteins exhibit very low levels of sequence similarity (15). The C-terminal region of VacA is a β -barrel domain that is required for secretion of VacA through an autotransporter (type V) pathway (19–21). Based on the sequence relatedness of the three VacA-like proteins to VacA within the β -barrel domain, it is presumed that the VacA-like proteins are also secreted by this route. Proteins secreted by the autotransporter pathway constitute the largest family of secreted proteins in Gram-negative bacteria (22–24). These proteins typically consist of three domains: (i) an N-terminal signal peptide, which is required for secretion across the inner membrane, (ii) a passenger domain, and (iii) a C-terminal β -domain, which facilitates translocation of the passenger domain across the outer membrane (15, 22–24). The passenger domains can have a wide variety of functions related to pathogenesis, including adhesion, autoaggregation, invasion, biofilm formation, and cytotoxicity. Structural analyses of several autotransporter passenger domains have revealed a conserved right-handed parallel β -helical fold (25–27). However, the primary amino acid sequences and specific functions of individual passenger domains are quite variable (22–24).

In the present study, we sought to learn more about the expression, subcellular localization, and *in vivo* roles of the VacA-like proteins. We show that all three *vacA*-like genes are expressed at increased levels when *H. pylori* colonizes the mouse stomach compared to *H. pylori* growth *in vitro*, and all three VacA-like proteins enhance the capacity of *H. pylori* to colonize the stomach. Studies of the localization of these proteins indicate that two VacA-like proteins localize in association with the bacterial body, whereas the third protein (which we designate FaaA, for flagella-associated autotransporter A) is detected as a component of the sheath overlying the flagellar filament and bulb. A *faaA* isogenic mutant exhibits decreased motility, decreased flagellar stability, and mislocalized flagella. Collectively, these results reveal that the localization of FaaA differs markedly from the localization of other known autotransporters and that FaaA has an important role in flagellar functions.

RESULTS

Detection of VacA-like proteins. *H. pylori* genomes contain three *vacA*-like genes, which are designated *imaA* (17), *faaA*, and *vlpC* (defined in Materials and Methods). These three genes, each >7 kb in length, are among the largest in the *H. pylori* genome. As a first step in analyzing the three VacA-like proteins, we genetically modified *H. pylori* strain 60190 to yield strains encoding c-Myc-tagged forms of each of these proteins. A schematic diagram of each of these proteins and sites of the c-Myc epitope tag insertion is shown in Fig. 1A. Western blot analysis with an anti-c-Myc antibody revealed that all three VacA-like proteins had a mass of >250 kDa (Fig. 1B). The relative intensity of the VlpC band was consistently lower than that of ImaA or FaaA, and the molecular mass of VlpC was smaller than that of the other VacA-like proteins (Fig. 1B). Genes encoding c-Myc-tagged versions of each VacA-like protein were also introduced into *H. pylori* strains J99 and X47, and Western blotting yielded results similar to those shown in Fig. 1B. Since the VacA-like proteins are predicted to be secreted by an autotransporter pathway, we hypothesized that these

proteins would be localized on the bacterial cell surface. To assess if this is indeed the case, we treated *H. pylori* strains producing c-Myc-tagged versions of ImaA, FaaA, and VlpC with proteinase K. Western blot analysis showed that all three VacA-like proteins and VacA were susceptible to proteinase K cleavage (Fig. 1C), whereas a negative-control protein (HspB) was not susceptible to proteinase K cleavage. This result provides evidence that all three VacA-like proteins are localized on the surface of *H. pylori*.

VacA is secreted as a soluble protein into the broth culture supernatant (10). To determine if the VacA-like proteins are secreted in a similar manner, *H. pylori* strains expressing c-Myc-tagged forms of these proteins were cultured in broth for 48 h, and intact bacteria were removed by centrifugation at $14,000 \times g$. ImaA and FaaA were detectable in the culture supernatant by Western blotting, but VlpC was not detected (data not shown), presumably because it was expressed at relatively low levels. To determine whether ImaA and FaaA are released into the culture supernatant as soluble proteins or in another form, preparations of culture supernatant were ultracentrifuged, which resulted in separation of soluble proteins from insoluble components. Western blot analysis indicated that ImaA and FaaA localized mainly to the insoluble fraction (see Fig. S1 in the supplemental material). Thus, in contrast to VacA, we did not detect secretion of VacA-like proteins as soluble proteins into the extracellular space. The presence of these proteins in the insoluble fraction of culture supernatant may be attributable to the release of outer membrane vesicles that contain these proteins (28).

Analysis of *imaA*, *faaA*, and *vlpC* *in vivo*. A previous study (using *H. pylori* strain G27) identified the *imaA* promoter as one of several promoters that are induced during *H. pylori* colonization of the mouse stomach compared to growth *in vitro* (6). Therefore, we hypothesized that the other *vacA*-like genes might be subject to similar regulation. C57BL/6 mice were orogastrically infected with *H. pylori* strain G27, and the animals were euthanized 2, 6, and 16 weeks thereafter. Transcription of *imaA*, *faaA*, and *vlpC* by *H. pylori* in the mouse stomach was analyzed by real-time reverse transcription-PCR (RT-PCR), as described in Materials and Methods. The transcription of all three genes was increased upon *H. pylori* colonization of the mouse stomach compared to *H. pylori* growth *in vitro* (Fig. 2A). The relative increase in transcription (*in vivo* compared to *in vitro*) was greatest for *imaA* at all three time points. These data confirm that *imaA* expression is increased during bacterial growth *in vivo* compared to bacterial growth *in vitro* and indicate that the other *vacA*-like genes also exhibit increased transcription *in vivo*.

A *vacA* mutant strain was previously reported to have a colonization defect compared to a wild-type strain in mouse infection experiments (29). To assess a potential role of VacA-like proteins *in vivo*, we performed competition experiments. Since *H. pylori* strain G27 colonized a relatively low proportion of challenged mice, we used *H. pylori* strain X47 for these experiments. Mice were coinfecting with 1:1 mixtures of the wild-type (WT) strain plus individual isogenic *imaA*, *faaA*, or *vlpC* mutants. After 2 weeks of infection, mice were euthanized, and bacterial colonization was assessed by analyzing bacterial growth on antibiotic-containing media that were selective for either the WT strain (metronidazole resistant) or the mutant strains (chloramphenicol resistant). The total bacterial densities in these animal stomachs ranged from 10^5 to 10^6 CFU/g for each animal; the bacterial densities did not differ significantly between animals challenged with

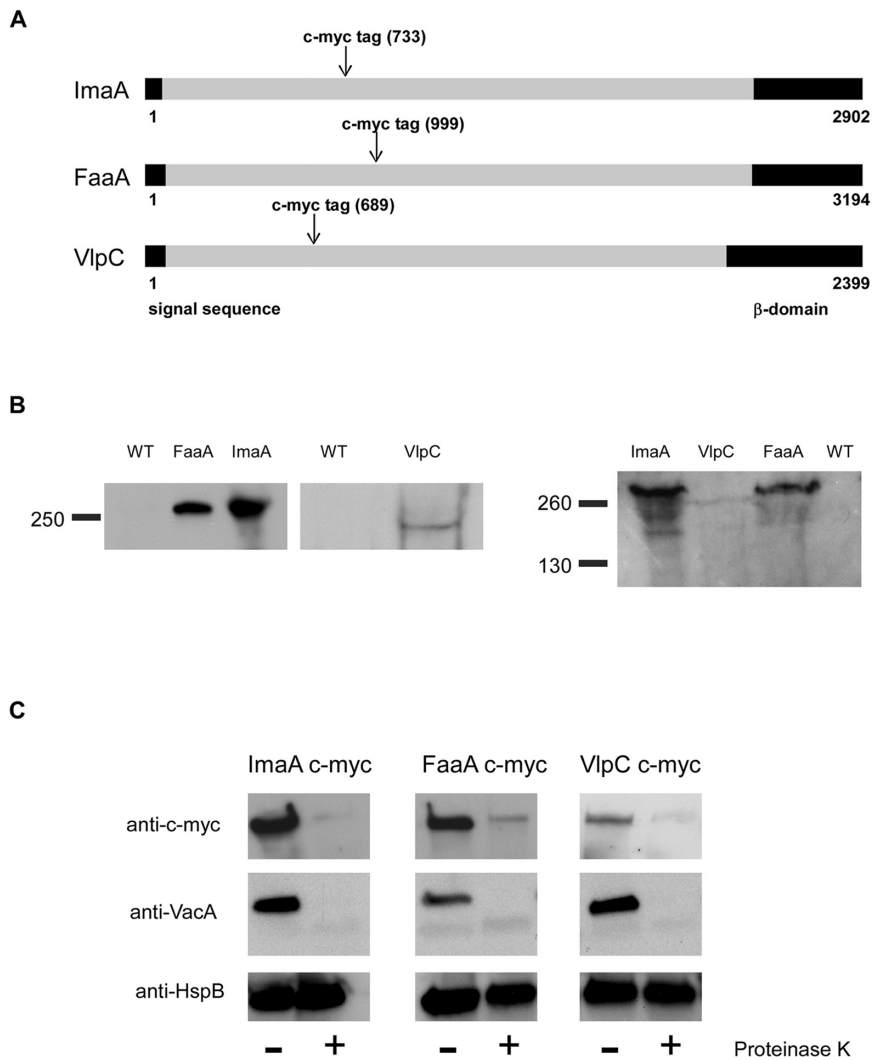


FIG 1 Detection of VacA-like proteins. (A) Schematic diagram of the three VacA-like proteins. Numbering corresponds to amino acid positions in the VacA-like proteins encoded by strain J99. Sites of c-Myc epitope tag insertion are shown. (B) *H. pylori* strain 60190 was engineered to encode c-Myc-tagged forms of the three VacA-like proteins. The WT strain and strains encoding c-Myc-tagged forms of FaaA, VlpC, or ImaA were grown overnight in broth culture, and production of each VacA-like protein was assessed by Western blot analysis using an anti-c-Myc antibody. All three proteins have masses of ≥ 250 kDa. (C) Strains encoding c-Myc-tagged forms of ImaA, FaaA, or VlpC were treated with 50 $\mu\text{g}/\text{ml}$ proteinase K or control buffer at 37°C for 30 min. Susceptibility of the three proteins to proteinase K cleavage was assessed by immunoblotting using an anti-c-Myc antibody. Cleavage of VacA and heat shock protein B (HspB) was monitored as a positive and negative control, respectively, using antisera against these proteins. The experiment was performed three times with similar results.

different strains. A competitive index was determined as described in Materials and Methods. The WT bacteria outcompeted all three mutant strains (Fig. 2B) ($P \leq 0.04$ for each mutant). Collectively, these experiments provide evidence that each of the VacA-like proteins has an important role *in vivo*.

Localization of FaaA to flagella. To further investigate the localization of the VacA-like proteins, we first utilized immunofluorescence microscopy to analyze *H. pylori* strains producing c-Myc-tagged versions of ImaA, FaaA, and VlpC. In these immunofluorescence studies, ImaA and VlpC were localized on the surfaces of the bacteria, as expected based on their sensitivity to proteinase K, and were localized to a bacterial pole (Fig. 3A to D). In

contrast, FaaA was localized to a site external to the bacterial body (Fig. 3E and F). Based on the immunofluorescence results, we hypothesized that FaaA might be localized to the flagella. To test this hypothesis, we generated preparations enriched in flagella from an *H. pylori* strain that produced a c-Myc tagged form of FaaA and from a control strain that produced a c-Myc-tagged form of ImaA. The presence of FaaA and ImaA in cell lysates and in the flagellar preparations was then examined by Western blotting using an anti-c-Myc antibody. As a control, we analyzed the presence of FlaA, the major flagellin subunit. As expected, FlaA was enriched in the flagellar preparations compared to total cell lysates (Fig. 3G), indicating an enrichment of flagellar components in the flagellar preparations. FaaA was also enriched in the flagellar preparations, whereas ImaA was not. These results support the hypothesis that FaaA is associated with flagella.

We then used immunoelectron microscopy to investigate potential flagellar localization of FaaA. *H. pylori* is characterized by the presence of multiple unipolar flagella (30, 31), and distinctive features of *H. pylori* flagella include the presence of a terminal bulb and a flagellar sheath (30–34). Analysis of FaaA localization by EM and immunogold staining revealed that FaaA localized to the flagellar sheath and the flagellar bulb (Fig. 4A to D). In contrast, ImaA, VlpC, and VacA were not detected in association with flagella (Fig. 4E to G) but were detected at the nonflagellar bacterial pole (see Fig. S2 in the supplemental material). Gold labeling was not detected in any of the negative-control samples; these included *H. pylori* lacking the c-Myc tag and processed in parallel with the other strains (Fig. 4H) and strains producing c-Myc-tagged versions of ImaA, FaaA, or VlpC that were immunolabeled with secondary antibody conjugated to gold particles alone (primary antibody omitted) (data not shown). Quantitative analyses confirmed that FaaA localizes mainly to the flagella (Table 1) ($P < 0.0001$). We also used immunofluorescence and electron microscopy to analyze two other *H. pylori* strains (J99 and X47) that produced c-Myc-tagged versions of ImaA, FaaA, and VlpC. Results in these strains were similar to what was observed in studies of strain 60190 and confirmed that FaaA localized to the flagella (Fig. 4D and data not shown).

Flagellar alterations in a *faaA* mutant strain. Since FaaA was localized to the flagella, we hypothesized that a *faaA* mutant strain might have a defect in flagellar morphology. To test this hypoth-

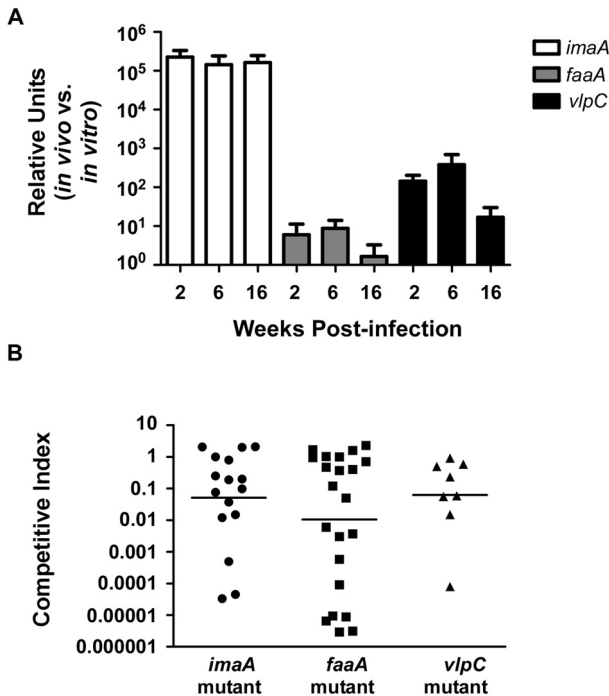


FIG 2 Analysis of *imaA*, *faaA*, and *vlpC* *in vivo*. (A) C57BL/6 mice were infected with *H. pylori* strain G27, and gene transcription was analyzed at 2, 6, or 16 weeks postinfection by real-time RT-PCR, as described in Materials and Methods. Expression of the indicated genes is given in relative units, and levels of gene expression in bacteria grown *in vitro* are assigned a value of 1. All three genes were expressed at higher levels *in vivo* than during bacterial growth *in vitro*. (B) Mice were inoculated with 1:1 mixtures of WT *H. pylori* X47 plus an *imaA* mutant ($n = 16$), WT plus a *faaA* mutant ($n = 22$), or WT plus a *vlpC* mutant ($n = 8$) for 2 weeks. The competitive index was calculated as described in Materials and Methods. Combined data from two independent experiments for FaaA and ImaA and one experiment for VlpC are shown, and each point represents the competitive index for one mouse stomach. WT bacteria out-competed *imaA*, *faaA*, and *vlpC* mutant bacteria, as indicated by competitive indices below 1 ($P \leq 0.04$ for each mutant, Student's *t* test). The horizontal lines represent the mean for each group.

esis, we performed transmission electron microscopy analyses of WT *H. pylori* strains, isogenic mutants, and mutants with restored alleles. Isogenic *vacA*, *imaA*, and *vlpC* mutants had flagellar morphologies similar to those of the respective WT *H. pylori* strains (60190, X47, and J99), with multiple flagella localized at the bacterial pole, as expected (Fig. 5A to D and data not shown). In contrast, the majority of the *faaA* mutant cells had flagellar defects, including absence of flagella, decreased numbers of flagella, or mislocalized flagella (Fig. 5E and F). The mislocalized flagella were found offset from the pole and at the lateral side of the bacterial cell body (Fig. 5E and F). In addition, preparations of the *faaA* mutants commonly contained broken flagella (Fig. 5E), which were rarely detected in preparations of the WT strain or other mutants; this suggests that the flagella produced by the *faaA* mutant might be more fragile than WT flagella. Introduction of an intact *faaA* allele into the *faaA* mutant reversed these alterations in flagellar localization and morphology (Fig. 5G). Quantitative analyses confirmed that there was a significant reduction in the number of intact flagella in the *faaA* mutant compared to the WT strain ($P < 0.0001$) and that there was a significantly increased number of nonpolar flagellar in this mutant (Fig. 5J, $P < 0.0001$).

In summary, these data indicate that FaaA contributes to flagellar stability and proper localization of flagella.

FaaA plays a role in flagellar stability. To further examine the role of FaaA in flagellar stability, we examined the production of FlaA (the major flagellin) in a WT strain, in isogenic *faaA*, *imaA* and *vlpC* mutants, and in a mutant with a restored *faaA* allele. In comparison to WT bacteria, *faaA* mutant bacteria produced reduced levels of FlaA, based on Western blot analysis (Fig. 6A). In a similar analysis of *imaA* and *vlpC* mutants compared to WT bacteria, there was no detectable difference in FlaA production (Fig. 6A). To investigate whether the observed reduction in FlaA protein production in the *faaA* mutant strain was due to a reduction in *flaA* transcription, we performed real-time RT-PCR analysis. We did not detect any decreased *flaA* transcription in the *faaA* mutant strain, but in fact, we detected increased *flaA* transcription in the *faaA* mutant compared to the WT strain (Fig. 6C) ($P < 0.03$). These results suggest that the reduced level of FlaA in a *faaA* mutant strain is due to reduced FlaA stability.

Decreased motility of *faaA* mutant strains. Since FaaA is localized to flagella and various flagellar alterations were detected in

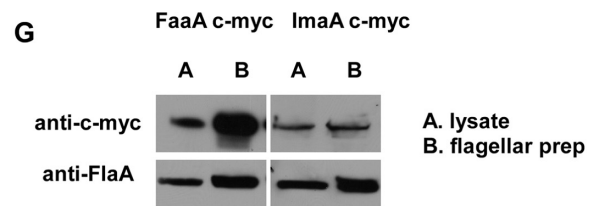
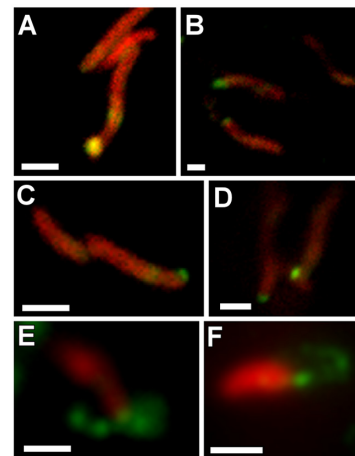


FIG 3 Analysis of the localization of VacA-like proteins. *H. pylori* strains were immunolabeled with monoclonal mouse anti-c-Myc antibody, followed by labeling with anti-mouse IgG conjugated to Alexa Fluor 488 (green channel). Bacterial cells were then counterstained as described in Materials and Methods (red channel) and visualized by fluorescence microscopy. The experiment was performed three times and a total of ≥ 200 bacteria were visualized for each experimental group. (A and B) *H. pylori* strain 60190 ImaA c-Myc; (C and D) *H. pylori* strain 60190 VlpC c-Myc; (E and F) *H. pylori* strain 60190 FaaA c-Myc. (G) A preparation enriched in flagella was prepared from *H. pylori* J99 strains that produced c-Myc-tagged FaaA or ImaA c-Myc. Samples were standardized by protein concentration, and the presence of c-Myc-tagged proteins in total cell lysates and in flagellar preparations was assessed by Western blotting. The presence of FlaA was assessed as a control. FaaA and FlaA were enriched in the flagellar preparations, whereas ImaA was not. The experiment was performed three times with similar results.

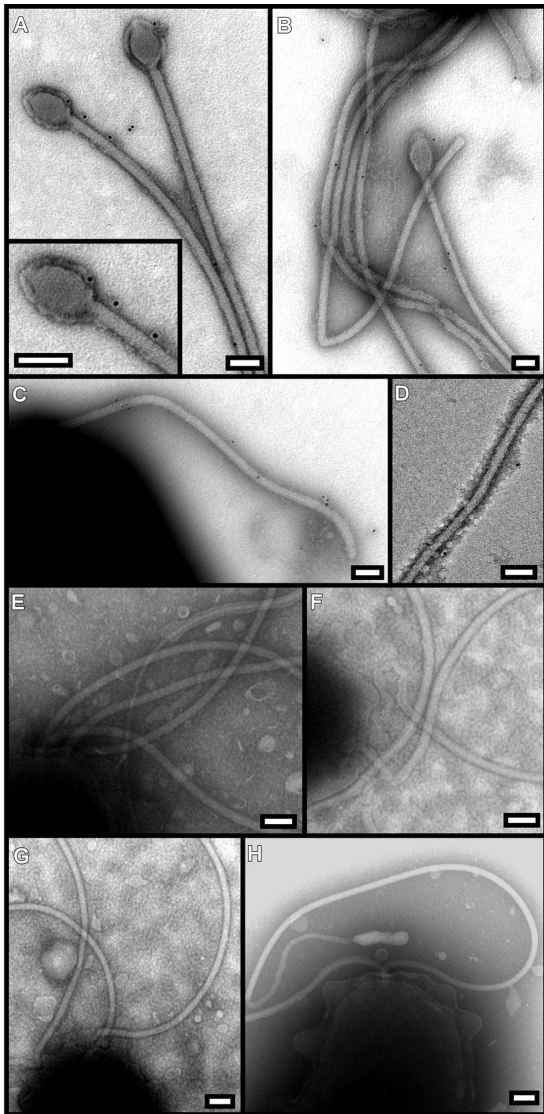


FIG 4 Immunogold EM analysis of FaaA localization. *H. pylori* strains were immunolabeled with primary antibodies to either VacA or c-Myc, followed by secondary antibodies conjugated to 10-nm immunogold particles. (A to C) 60190 FaaA c-Myc labeled with an anti-c-Myc antibody, demonstrating FaaA localization to the flagellar filament and flagellar bulb. (D) X47 FaaA c-Myc labeled with an anti-c-Myc antibody; (E) 60190 ImaA c-Myc labeled with an anti-c-Myc antibody; (F) 60190 (no c-Myc tag) labeled with an anti-VacA antibody; (G) 60190 VlpC c-Myc labeled with an anti-c-Myc antibody; (H) 60190 (no c-Myc tag) labeled with an anti-c-Myc antibody. FaaA localizes to flagella, whereas VacA, ImaA, and VlpC do not. The experiment was performed three times in multiple strains with similar results. Bars, 100 nm.

faaA mutant strains, we hypothesized that FaaA might be required for optimal *H. pylori* motility. To test this hypothesis, we analyzed the motility of a WT strain, a *faaA* isogenic mutant, and a mutant with a restored intact copy of *faaA*. In comparison to the WT strain, the *faaA* mutant strain exhibited decreased motility (Fig. 7A). Restoration of an intact *faaA* gene reversed the defect in motility (Fig. 7A). There were no significant differences in the motility of *imaA* or *vlpC* mutants compared to the WT strain (Fig. 7B). These results indicate that FaaA is required not only for flagellar stability and proper flagellar localization but also for optimal motility.

Role of FaaA in *H. pylori* colonization of the mouse stomach.

Competition experiments showed that a strain containing intact VacA-like proteins has a competitive advantage over a *faaA* mutant strain, based on analysis at two weeks postinfection (Fig. 2). To further investigate the role of *faaA* *in vivo*, we orogastrically infected C57BL/6 mice with either the WT strain alone or an isogenic *faaA* mutant strain alone. Mice were euthanized, and colonization of the stomach was analyzed at 4 days or 1 month postinfection. At 4 days postinfection, the *faaA* mutant strain demonstrated attenuated colonization compared to the WT strain (Fig. 8A) ($P = 0.0172$). In contrast, there was no significant difference at 1 month postinfection (Fig. 8B). These data, along with the competition experiments (Fig. 2), indicate that FaaA is required for optimal *H. pylori* colonization during early stages of infection, when flagella are required for bacterial entry into the gastric mucus layer (35, 36).

DISCUSSION

The *H. pylori* genome contains three *vacA*-like genes that have C-terminal regions related to that of *vacA*, which encodes a secreted toxin. The C-terminal regions shared by VacA and the VacA-like proteins correspond to a predicted β -barrel domain that is required for protein secretion via the autotransporter pathway. The results of the present study show that these three VacA-like proteins share several common features. ImaA, FaaA, and VlpC are among the largest proteins produced by *H. pylori* (each >250 kDa in mass), and they are each localized on the bacterial surface. The three *vacA*-like genes are all upregulated during *H. pylori* colonization of the mouse stomach compared to *H. pylori* growth *in vitro*. Finally, *imaA*, *faaA*, and *vlpC* mutants each have a competitive disadvantage compared to the WT strain in mouse colonization experiments.

Unlike ImaA and VlpC, which are localized to a bacterial pole, FaaA is localized to the flagella. Correspondingly, *faaA* mutants exhibit multiple flagellar abnormalities, including absence of flagella, decreased numbers of flagella, increased flagellar fragility, and mislocalization of flagella to the lateral side of the bacteria instead of the pole. In addition, *faaA* mutant bacteria exhibit decreased motility compared to the WT strain. Thus, FaaA is required not only for flagellar stability and proper flagellar localization but also for optimal flagellar function. In an analysis of gastric colonization, a *faaA* mutant strain colonized the mouse stomach less efficiently than WT bacteria at an early time point postinfection, which is consistent with a known essential role of motility at early stages of *H. pylori* infection (36). FaaA might also have a role at later stages of infection, since flagella are likely to be required for continuous *H. pylori* colonization of the gastric mucus layer during the natural turnover of gastric mucus and exfoliation of gastric epithelial cells.

To the best of our knowledge, flagellar localization of autotransporter proteins has not previously been reported. The atypical localization of FaaA is probably attributable at least in part to unusual features of *H. pylori* flagella. *H. pylori* contains 2 to 6 polar flagella that are characterized by the presence of a sheath and a terminal bulb (30–34). Thus far, there has been relatively little analysis of the *H. pylori* flagellar sheath, and only one protein, HpaA, has been previously localized to this site (37–39). We speculate that the flagellar sheath contains multiple components that are derived from the *H. pylori* outer membrane. Therefore, we propose that FaaA is exported to the outer membrane and subse-

TABLE 1 Analysis of FaaA localization^{a,b}

Strain	Mean no. of gold particles per bacterium at site			Side of bacterium
	Flagella	Flagellar pole	Nonflagellar pole	
60190 FaaA c-Myc	2.7 ± 0.5	0.87 ± 0.18	0	0.56 ± 0.0.13
60190 <i>faaA</i> mutant	0	0	0	0
60190	0	0	0	0.028 ± 0.17

^a FaaA localization in the indicated strains was analyzed by immunogold EM, using an anti-c-Myc antibody followed by a secondary antibody conjugated to immunogold particles. Mean ± SEM values are reported.

^b The numbers of bacteria that were analyzed to generate the data were 45 for 60190 FaaA c-Myc, 123 for the 60190 *faaA* mutant, and 37 for 60190.

quently becomes a component of the flagellar sheath. Interestingly, we noted that levels of FlaA (the major component of flagella) were diminished in a *faaA* mutant, but there was no detectable reduction in *flaA* transcription in this mutant. We hypothesize that FaaA interacts directly or indirectly with multiple flagellar proteins; thus, the absence of FaaA may result in decreased protein stability of FlaA and possibly decreased stability of other flagellar components as well.

In summary, this study highlights important features of the *H. pylori* VacA-like proteins, including upregulation of the corresponding genes *in vivo* and a role for these proteins in colonization of the mammalian stomach. Unexpectedly, we show that one of these proteins, FaaA, localizes to flagella and that FaaA is required for proper flagellar localization and optimal flagellar function. This unusual localization and function of an autotransporter protein presumably reflects an adaptation designed to optimize *H. pylori* colonization of the gastric mucosal niche.

MATERIALS AND METHODS

Bacterial strains and culture conditions. *H. pylori* strains 60190 (ATCC 49503), 60190 *vacA::cat-rdxA* (40), and J99 (ATCC 700824) and mouse-adapted versions of strain G27 and X47 were selected for use in this study. *H. pylori* strains were routinely grown at 37°C on Trypticase soy agar plates containing 5% sheep blood in ambient air containing 5% CO₂. *H. pylori* mutant strains were selected based on resistance to chloramphenicol (2.5 μg ml⁻¹) or resistance to metronidazole (7.5 μg ml⁻¹) on brucella agar plates (brucella broth containing 1.35% agar and 10% fetal bovine serum [FBS]). *H. pylori* liquid cultures were grown in brucella broth (Sigma) supplemented with 5 to 10% fetal bovine serum (Atlanta Biologicals) or cholesterol (Gibco) (41). Prior to mouse infections, *H. pylori* strains were grown in brucella broth containing 10% FBS and 10 μg ml⁻¹ vancomycin at 37°C under microaerobic conditions generated by a GasPakEZ Campy Container System (BD Biosciences).

Mutagenesis of *imaA*, *faaA*, and *vlpC* and production of c-Myc-tagged proteins. In this present study, we designate HP0289/JHP0274 as *ImaA* (for immunomodulatory autotransporter protein A [17]), HP0609/JHP0556 as *FaaA* (for flagella-associated autotransporter A), and HP0922/JHP0856 as *VlpC* (for VacA-like protein C). To introduce mutations into these genes, we used a previously described mutagenesis method (42, 43). As a first step, metronidazole-resistant forms of strains 60190, X47, and J99 (60190Δ*rdxA*, X47Δ*rdxA*, and J99Δ*rdxA*) were generated by deleting the *rdxA* gene (43). Next, fragments of each gene (nucleotides 1,261 to 3,530 for *imaA*, 2,041 to 4,284 for *faaA*, and 1,390 to 3,639 for *vlpC*, with numbers based on the DNA sequences from *H. pylori* strain J99) were PCR amplified from *H. pylori* 60190, X47, and J99 genomic DNA and cloned into pGEM-T Easy (Promega). These plasmids were then used as templates for inverse PCR to generate modified plasmids containing a BamHI site after nucleotide 2199, 2997, and 2067 (numbers based on the sequences of genes in *H. pylori* strain J99) in *imaA*, *faaA*, and *vlpC*, respectively. The locations of the BamHI sites were selected based on the identification of regions that are predicted to be surface-exposed in a Hopp-Woods hydrophobicity analysis ([\[.vivo.colostate.edu/molkit/hydrophathy/\]\(http://www.colostate.edu/molkit/hydrophathy/\)\). A *cat-rdxA* cassette was cloned into the BamHI site, and *cat-rdxA*-containing plasmids, which are unable to replicate in *H. pylori*, were then transformed into *H. pylori* 60190Δ*rdxA*, X47Δ*rdxA*, and J99Δ*rdxA*, thereby allowing insertion of the *cat-rdxA* cassette into *imaA*, *faaA*, or *vlpC*. Single colonies were selected based on chloramphenicol resistance and metronidazole sensitivity. In each case, correct insertion of the *cat-rdxA* cassette was confirmed by PCR analysis.](http://www</p>
</div>
<div data-bbox=)

To restore an intact copy of the relevant gene in strains that had been mutated and simultaneously insert a sequence encoding a c-Myc epitope tag into the gene of interest, we used a counterselection method, as described previously (42, 43). A DNA sequence encoding a c-Myc tag (5' GAA CAA AAA CTT ATT AGT GAA GAA GAT CTT 3') was inserted into the BamHI site in the plasmids described above using a QuikChange II XL site-directed mutagenesis kit (Agilent). Correct insertion of the c-Myc tag was confirmed by DNA sequencing. Plasmids containing the c-Myc-tagged versions of each VacA-like protein were then transformed into the appropriate *H. pylori* strains containing the *cat-rdxA* cassette, and metronidazole-resistant transformants were selected. This resulted in replacement of the *cat-rdxA* cassette with a sequence that contained the c-Myc tag.

Experiments in this study analyzed properties of metronidazole-resistant strains that contain WT copies of *imaA*, *faaA*, and *vlpC*, compared to isogenic mutant strains with disruptions of *imaA*, *faaA*, and *vlpC* and derivatives that contain restored intact forms of these genes with a c-Myc epitope tag. For convenience, the parental strains are designated WT here (despite the presence of the *rdxA* mutation) because they contain WT copies of all three *vacA*-like genes.

Detection of c-Myc-tagged proteins. The presence of c-Myc-tagged VacA-like proteins was assessed by Western blot analysis using an anti-c-Myc antibody (4F6, 1:1,000; Vanderbilt Monoclonal Antibody Core) followed by a horseradish peroxidase (HRP)-conjugated secondary antibody (1:10,000; Promega). Proteins were visualized by incubation with chemiluminescent substrate solution (Pierce) and exposure to X-ray film.

Proteinase K susceptibility. The susceptibility of the VacA-like proteins to proteinase K digestion was assessed using a modified version of previous protocols (43, 44). *H. pylori* strains were grown in liquid medium for 18 h and then harvested and washed with PBS. Bacteria were then resuspended in RPMI medium only or RPMI medium containing 50 μg/ml of proteinase K and incubated at 37°C for 30 min. Proteinase K activity was abrogated by the addition of phenylmethylsulfonyl fluoride (PMSF; 2 mM final concentration). The bacteria were washed in RPMI containing 2 mM PMSF, resuspended in SDS sample buffer, and analyzed by immunoblotting using an anti-c-Myc antibody. As controls, we monitored proteolysis of VacA, which is known to be localized to the bacterial surface (13), and heat shock protein B (HspB), which is localized within the cytoplasm, using antisera directed toward these proteins. Antibody concentrations used were 1:1,000 (anti-c-Myc), 1:10,000 (anti-VacA), and 1:20,000 (anti-HspB).

Immunofluorescence microscopy. *H. pylori* strains were washed in PBS (pH 7.4), fixed in PBS containing 2.5% glutaraldehyde and 2.0% paraformaldehyde for 1 h at room temperature, washed twice with PBS, and blocked for 1 h in PBS containing 0.1% bovine serum albumin. Cells were incubated with

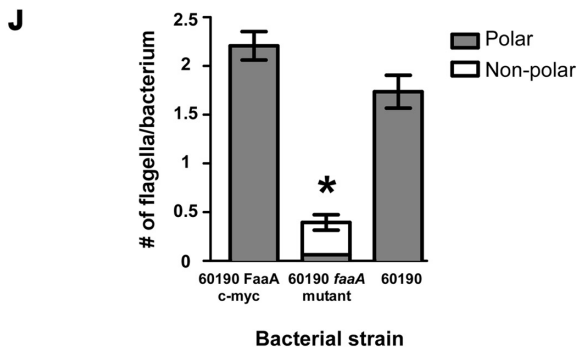
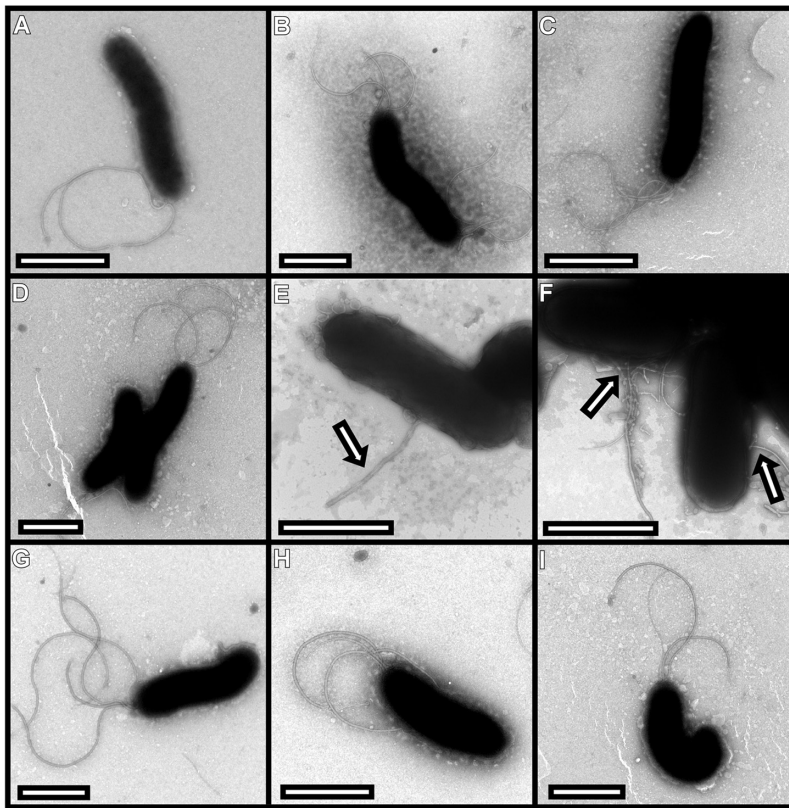


FIG 5 Analysis of flagellar morphology and localization. *H. pylori* strains were analyzed by transmission EM and negative staining, as described in Methods. (A) Strain 60190 (without c-Myc tag); (B) 60190 *imaA* mutant; (C) 60190 *ImaA* c-Myc; (D) 60190 *vacA*-null mutant; (E) 60190 *faaA* mutant; (F) X47 *faaA* mutant; (G) 60190 *FaaA* c-Myc; (H) 60190 *vlpC* mutant; (I) 60190 *VlpC* c-Myc. Mislocalized flagella (arrows) were detected in the *faaA* mutant strains but not in the other mutants. The experiment was performed three times in multiple strains with similar results. Bars, 1 μm . (J) Graph showing quantification of the number of flagella per bacterium (based on analysis of 87 bacteria for 60190 *FaaA* c-Myc, 64 bacteria for the 60190 *faaA* mutant, and 19 bacteria for WT 60190). *faaA* mutant bacteria had significantly fewer flagella per bacterium than either WT bacteria or the mutant with restored *faaA* (asterisk, $P < 0.0001$, Kruskal-Wallis test). In addition, the *faaA* mutant strain had a significantly increased number of nonpolar flagella compared to WT bacteria or the mutant with restored *faaA* ($P < 0.0001$, Kruskal-Wallis test).

anti-c-Myc antibody for 4 h at 4°C. Afterward, cells were washed three times with PBS and then incubated overnight at 4°C with an Alexa Fluor 488-conjugated secondary antibody (goat anti-mouse IgG; Invitrogen). Bacterial cells were washed three times with PBS before being counterstained with propidium iodide. As negative controls, replicate samples were processed by

applying secondary antibodies alone. Samples were mounted using ProLong Gold antifade reagent (Invitrogen) and viewed using a Zeiss Axioptot wide-field microscope or a Zeiss LSM710 confocal laser scanning microscope.

Immunoelectron microscopy. Immunoelectron microscopy was performed as described previously (43). Briefly, *H. pylori* strains were washed in 0.05 M sodium cacodylate buffer (pH 7.4) and then fixed in 2.5% glutaraldehyde and 2.0% paraformaldehyde in 0.05 M sodium cacodylate buffer for 1 h at room temperature. Cells were washed twice with sodium cacodylate buffer and blocked for 1 h in sodium cacodylate buffer containing 0.1% gelatin. Cells were incubated with primary antibody (mouse monoclonal anti-c-Myc) for 4 h at 4°C. Afterward, cells were washed three times with sodium cacodylate buffer before incubation overnight at 4°C with goat anti-mouse IgG conjugated to 10 nm gold particles (Ted Pella) or 25 nm gold particles (Electron Microscopy Sciences). The following day, bacterial cells were spotted onto Formvar-coated grids (Electron Microscopy Sciences) and negatively stained with 1% ammonium molybdate. As negative controls, replicate samples were processed by applying secondary antibodies alone. Samples were viewed with a FEI T-12 or a Philips C-12 transmission electron microscope. *FaaA* labeling and localization were quantified by counting the number of gold particles. Quantitation was done by one person (J.N.R.), who was blinded to the identity of the samples.

Electron microscopy analysis of flagella. *H. pylori* strains were cultured on blood agar plates or in brucella broth (BB)-5% FBS overnight at 37°C in 5% CO₂. Cells were harvested from the plate in 0.05 M sodium cacodylate buffer (pH 7.4) for an initial wash. Bacterial cells were spotted onto Formvar-coated grids and negatively stained with 1% ammonium molybdate. Samples were viewed with a FEI T-12 or a Philips C-12 transmission electron microscope. The number and localization of flagella were quantified by counting the number of flagella per bacterium. Quantification was done by one person (J.N.R.), who was blinded to the identity of the samples.

Motility assay. *H. pylori* motility was analyzed as described previously (36, 45). Briefly, 1- μl aliquots of bacterial suspensions (overnight broth cultures back-diluted to an optical density at 600 nm [OD₆₀₀] of 0.1) were stabbed into soft agar plates composed of BB-10% FBS and 0.35% agar. The plates were then incubated for 5 days at 37°C in 5% CO₂, and the diameters of the bacterial halos were measured each day.

Enrichment of flagella. A preparation enriched in flagella was prepared using a protocol adapted from previously described methods (46-48). Briefly, *H. pylori* strains were grown in liquid culture at 37°C for 18 h under microaerobic conditions. Bacteria were centrifuged at 6,000 rpm for 10 min, pellets were resuspended in sucrose solution (0.5 M sucrose, 10 mM Tris-HCl [pH 8.0]) containing lysozyme (0.02 mg/ml final concentration), EDTA (10 mM final concentration), and Zwitter-

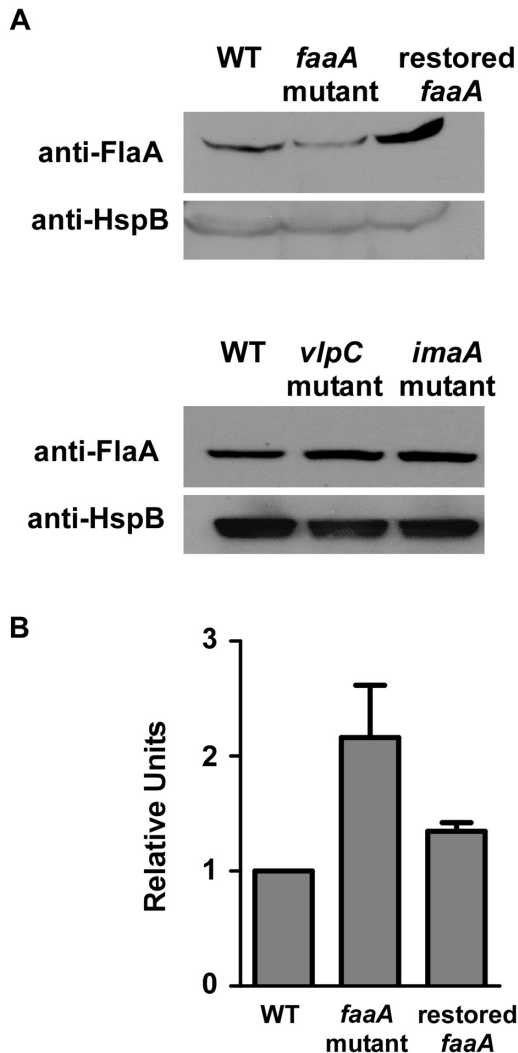


FIG 6 FaaA has a role in flagellar stability. (A) WT *H. pylori* strain J99, isogenic *faaA*, *vlpC*, and *imaA* mutant strains, and a *faaA* mutant with a restored intact *faaA* allele were cultured overnight in BB-FBS, and the presence of FlaA was assessed by Western blotting. The presence of HspB was monitored as a control. The level of FlaA was reduced in the *faaA* mutant compared to the other strains. The experiment was performed multiple times with similar results. (B) Transcription of *flaA* was analyzed by real-time RT-PCR, as described in Materials and Methods. RNA from WT bacteria served as the calibrator, and relative units are shown in comparison to the WT strain. Transcription of *flaA* was increased in the *faaA* mutant strain compared to the WT strain. Error bars represent mean plus standard error from combined results of three independent experiments performed in triplicate.

gent (2 mg/ml final concentration), and the suspensions were incubated at 4°C for 4 to 6 h with gentle shaking. Suspensions were then centrifuged at 25,000 × *g* for 30 min and pellets containing the flagella were resuspended in 5 ml PBS. Flagellar preparations were examined by Western blot analysis using anti-c-Myc (4F6; Vanderbilt Monoclonal Antibody Core) and anti-FlaA (Fisher) antibodies (each at a 1:1,000 dilution), followed by appropriate HRP-conjugated secondary antibodies.

RNA isolation and analysis of gene expression by real-time RT-PCR. Total RNA was isolated from *H. pylori* using TRI reagent solution (Ambion) according to the manufacturer's instructions, with slight modifications. Bacterial pellets were resuspended in TRI reagent solution, and one chloroform extraction was performed. The RNA was then mixed with 70% ethanol and purified using an RNeasy minikit (Qiagen). RNA sam-

ples were DNase treated using DNA-free (Ambion). RNA was then reverse transcribed using a high-capacity RNA-to-cDNA kit (Applied Biosystems). As a control, samples were processed without reverse transcriptase. The cDNA and control reactions were diluted 1:10 and used in real-time RT-PCR reactions. Real-time RT-PCR was performed using a Step One Plus real-time PCR machine (Applied Biosystems), with SYBR green as the fluorochrome. Abundance of transcript was calculated using the $\Delta\Delta C_T$ method, with each transcript signal normalized to 16S rRNA. Transcript signals for each experimental sample were then compared to transcript signals from control bacteria grown *in vitro*. Primer sequences were as follows: *imaA*, 5' GACACCAATAGCGCGGTTGT 3' and 5' TCAGCCGAGCTGGACTCTAAA 3'; *faaA*, 5' GATAACGGCTTGACTTACATCAAAA 3' and 5' CACGGTGTACTGGCGTTGT 3'; *vlpC*, 5' TGGCGACAGGAGTTGGA 3' and 5' TTGCATGAAACCCGCTATACC 3'; *flaA*, 5' CATGGGGATTATCCAGTTG 3' and 5' CGATACGAACC TGACCGATT 3'; 16S rRNA, 5' CTAGCGGATTCTCTCAATGTCAA 3' and 5' GGAGTACGGTCGCAAGATTTAAA 3'.

Infection of mice with *H. pylori*. Eight-week-old *Helicobacter*-free male C57BL/6 mice (Jackson Laboratory) were used in all experiments, with a minimum of 5 to 10 mice per group. Prior to infection of mice, *H. pylori* was inoculated into liquid medium and cultured for 18 h under microaerobic conditions. Mice were orogastrically inoculated with a suspension of 5 × 10⁸ CFU of *H. pylori* in 0.5 ml of brucella broth without supplemental FBS (49). For competition experiments, mice were coinfecting with a 1:1 ratio of the WT strain plus *imaA*, *faaA*, or *vlpC* mutant *H. pylori* strains, using a total input of approximately 5 × 10⁸ CFU in 0.5 ml of brucella broth. The inocula of the WT and mutant strains used for coinfection experiments were verified to contain equivalent CFU/ml, based on colony counting. Mice were orogastrically infected with two doses, administered two days apart. For *in vivo* gene expression studies, mice were euthanized at 2, 6, and 16 weeks postinfection. For competition experiments, mice were euthanized at 2 weeks postinfection. For colonization studies in which animals were infected with a single strain, mice were euthanized at 4 days or 1 month postinfection.

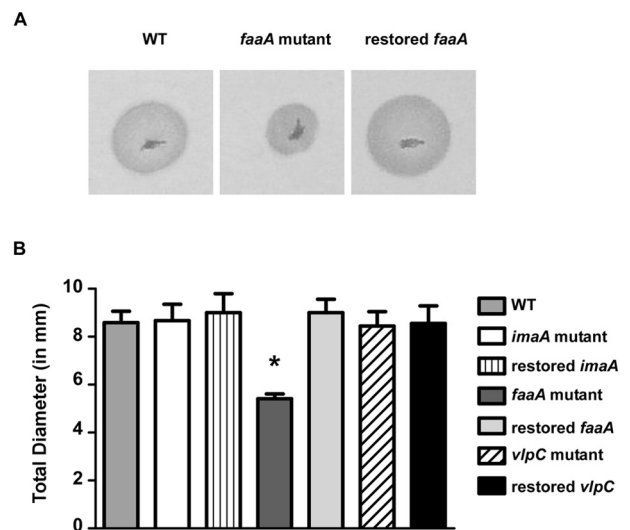


FIG 7 Mutation of *faaA* results in decreased motility. Motility of WT *H. pylori* strain J99, isogenic *imaA*, *faaA*, and *vlpC* mutant derivatives, and mutants with restored intact forms of *imaA*, *faaA*, and *vlpC* was assessed. Bacterial suspensions were inoculated into semisolid brucella medium, and the outward migration was measured over a period of 5 days. (A) Analysis of the motility of a *faaA* mutant compared to the WT strain and a mutant with a restored intact *faaA*. (B) Quantification of *H. pylori* motility. The motility of the *faaA* mutant was significantly decreased compared to that of the WT strain and the other strains tested. Data are means plus standard errors from combined results of three independent experiments, each performed in triplicate. The asterisk indicates a *P* value of <0.05 compared to all other strains (Student's *t* test).

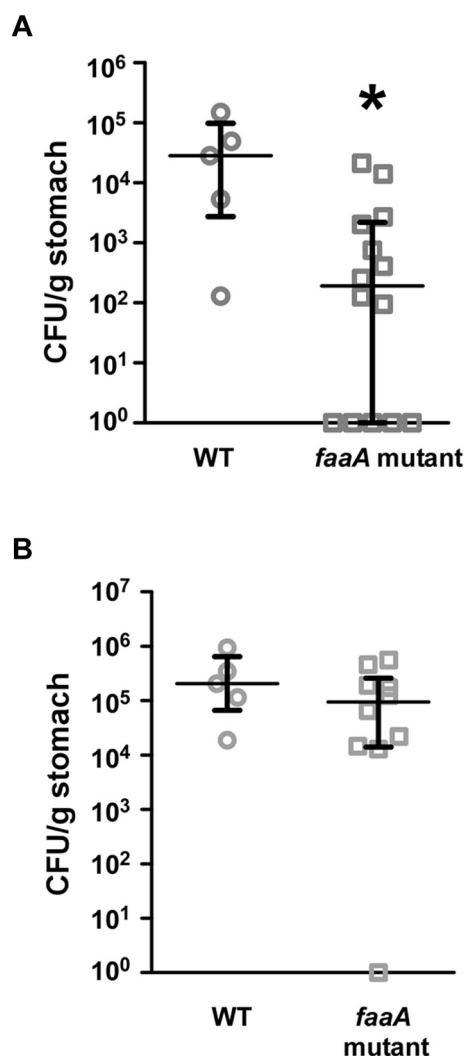


FIG 8 Role of FaaA in *H. pylori* colonization of the mouse stomach. C57BL/6 mice were infected with WT *H. pylori* strain X47 or an isogenic mutant for 4 days or 1 month. Mice were then euthanized and *H. pylori* colonization of the stomach was analyzed as described in Materials and Methods. (A) C57BL/6 mice were orogastrically infected with either the WT strain or an isogenic *faaA* mutant strain (WT, $n = 5$; *faaA* mutant, $n = 14$) for 4 days. The asterisk indicates a P value of 0.019 (Mann-Whitney U test). (B) Mice were infected with the WT strain or a *faaA* mutant strain (WT, $n = 5$; *faaA* mutant, $n = 10$) for 1 month. CFUs for individual mice are shown. Medians with interquartile ranges are shown.

Processing of mouse stomachs and culturing of *H. pylori* from mouse stomachs. Mouse stomachs were processed as described previously, with minor modifications (49). The stomach was removed from each mouse by excising between the esophagus and the duodenum. The forestomach (nonglandular stomach) was removed from the glandular stomach and discarded. The glandular stomach was opened and rinsed gently in PBS. For colonization studies, the glandular stomach was cut in half and placed into brucella broth for immediate processing. Gastric tissue was then homogenized using a Tissue Tearor (BioSpec Products), and serial dilutions of the homogenate were plated on Trypticase soy agar plates containing 5% sheep blood, $10 \mu\text{g ml}^{-1}$ nalidixic acid, $100 \mu\text{g ml}^{-1}$ vancomycin, $2 \mu\text{g ml}^{-1}$ amphotericin, and $200 \mu\text{g ml}^{-1}$ bacitracin. For coinfection experiments, plates also contained either chloramphenicol ($2.5 \mu\text{g ml}^{-1}$) or metronidazole ($7.5 \mu\text{g ml}^{-1}$), in order to permit selective

isolation of mutant and WT strains, respectively (the WT strain X47 used in these experiments is metronidazole resistant, and the *imaA*, *faaA*, and *vlpC* mutants are chloramphenicol resistant). Plates were cultured under microaerobic conditions for 5 days before colonies were counted.

For experiments designed to analyze bacterial transcription *in vivo*, stomachs were incised and washed as described above, the gastric mucosa was scraped with cell scrapers (Fisher), and the scraped mucosa was placed in RNAprotect (Qiagen). Scrapings from 3 or 4 mouse stomachs were combined and analyzed as a single pooled sample. RNA was isolated and RT-PCR was performed as described above. Competitive index was determined by dividing the number of cultured mutant bacteria by the number of cultured WT bacteria, followed by corrections for any deviations from an input ratio of 1:1 (17).

Statistical analysis. Gene transcription data, motility data, mouse colonization data, competition data, and flagellar localization data were analyzed using Student's t test. Bacterial colonization densities were analyzed using the Mann-Whitney U test. Quantitative data pertaining to FaaA labeling, flagellar numbers, and flagellar localization were analyzed using the Kruskal-Wallis test. All statistical analyses were performed using the GraphPad Prism 5 program.

Ethics statement. This study was carried out in strict accordance with the recommendations in the Guide for the Care and Use of Laboratory Animals of the National Institutes of Health. The protocol was approved by the Institutional Animal Care and Use Committee of Vanderbilt University School of Medicine and the VA Institutional Animal Care and Use Committee (V/10/157 and M/06/333).

SUPPLEMENTAL MATERIAL

Supplemental material for this article may be found at <http://mbio.asm.org/lookup/suppl/doi:10.1128/mBio.00613-12/-/DCSupplemental>.

Figure S1, TIF file, 0.7 MB.

Figure S2, TIF file, 7.3 MB.

ACKNOWLEDGMENTS

This study is based on work supported by NIH AI039657, CA116087, AI068009, F32 AI102568, T32 AI007281, and the Department of Veterans Affairs, Veterans Health Administration, Office of Research and Development. Experiments in the Vanderbilt Cell Imaging Shared Resource were supported by the Vanderbilt University Digestive Disease Research Center (NIH grant P30DK058404) and the Vanderbilt University Ingram Cancer Center.

We thank Mark S. McClain for helpful discussions. We thank David Hendrixson and Deborah Ribardo at UT Southwestern Medical Center for advice on methods for flagellar enrichment. We thank Tatsuki Koyama for advice on statistical analyses.

REFERENCES

- Amieva MR, El-Omar EM. 2008. Host-bacterial interactions in *Helicobacter pylori* infection. *Gastroenterology* 134:306–323.
- Atherton JC, Blaser MJ. 2009. Coadaptation of *Helicobacter pylori* and humans: ancient history, modern implications. *J. Clin. Invest.* 119:2475–2487.
- Cover TL, Blaser MJ. 2009. *Helicobacter pylori* in health and disease. *Gastroenterology* 136:1863–1873.
- Suerbaum S, Michetti P. 2002. *Helicobacter pylori* infection. *N Engl J. Med.* 347:1175–1186.
- Blaser MJ, Berg DE. 2001. *Helicobacter pylori* genetic diversity and risk of human disease. *J. Clin. Invest.* 107:767–773.
- Castillo AR, Woodruff AJ, Connolly LE, Sause WE, Otemann KM. 2008. Recombination-based *in vivo* expression technology identifies *Helicobacter pylori* genes important for host colonization. *Infect. Immun.* 76:5632–5644.
- de Bernard M, Cappon A, Del Giudice G, Rappuoli R, Montecucco C. 2004. The multiple cellular activities of the VacA cytotoxin of *Helicobacter pylori*. *Int. J. Med. Microbiol.* 293:589–597.
- Fischer W, Prassl S, Haas R. 2009. Virulence mechanisms and persis-

- tence strategies of the human gastric pathogen *Helicobacter pylori*. *Curr. Top. Microbiol. Immunol.* 337:129–171.
9. Kim IJ, Blanke SR. 2012. Remodeling the host environment: modulation of the gastric epithelium by the *Helicobacter pylori* vacuolating toxin (VacA). *Front. Cell. Infect. Microbiol.* 2:37.
 10. Cover TL, Blaser MJ. 1992. Purification and characterization of the vacuolating toxin from *Helicobacter pylori*. *J. Biol. Chem.* 267:10570–10575.
 11. Cover TL, Tummuru MK, Cao P, Thompson SA, Blaser MJ. 1994. Divergence of genetic sequences for the vacuolating cytotoxin among *Helicobacter pylori* strains. *J. Biol. Chem.* 269:10566–10573.
 12. Cover TL, Blanke SR. 2005. *Helicobacter pylori* VacA, a paradigm for toxin multifunctionality. *Nat. Rev. Microbiol.* 3:320–332.
 13. Ilver D, Barone S, Mercati D, Lupetti P, Telford JL. 2004. *Helicobacter pylori* toxin VacA is transferred to host cells via a novel contact-dependent mechanism. *Cell. Microbiol.* 6:167–174.
 14. Alm RA, Ling LS, Moir DT, King BL, Brown ED, Doig PC, Smith DR, Noonan B, Guild BC, deJonge BL, Carmel G, Tummino PJ, Caruso A, Uria-Nickelsen M, Mills DM, Ives C, Gibson R, Merberg D, Mills SD, Jiang Q, Taylor DE, Vovis GF, Trust TJ. 1999. Genomic-sequence comparison of two unrelated isolates of the human gastric pathogen *Helicobacter pylori*. *Nature* 397:176–180.
 15. Tomb JF, White O, Kerlavage AR, Clayton RA, Sutton GG, Fleischmann RD, Ketchum KA, Klenk HP, Gill S, Dougherty BA, Nelson K, Quackenbush J, Zhou L, Kirkness EF, Peterson S, Loftus B, Richardson D, Dodson R, Khalak HG, Glodek A, McKenney K, Fitzgerald LM, Lee N, Adams MD, Hickey EK, Berg DE, Gocayne JD, Utterback TR, Peterson JD, Kelley JM, Cotton MD, Weidman JM, Fujii C, Bowman C, Watthey L, Wallin E, Hayes WS, Borodovsky M, Karp PD, Smith HO, Fraser CM, Venter JC. 1997. The complete genome sequence of the gastric pathogen *Helicobacter pylori*. *Nature* 388:539–547.
 16. Kavermann H, Burns BP, Angermuller K, Odenbreit S, Fischer W, Melchers K, Haas R. 2003. Identification and characterization of *Helicobacter pylori* genes essential for gastric colonization. *J. Exp. Med.* 197:813–822.
 17. Sause WE, Castillo AR, Ottemann KM. 2012. The *Helicobacter pylori* autotransporter ImaA (HP0289) modulates the immune response and contributes to host colonization. *Infect. Immun.* 80:2286–2296.
 18. Baldwin DN, Shepherd B, Kraemer P, Hall MK, Sycuro LK, Pinto-Santini DM, Salama NR. 2007. Identification of *Helicobacter pylori* genes that contribute to stomach colonization. *Infect. Immun.* 75:1005–1016.
 19. Fischer W, Buhrdorf R, Gerland E, Haas R. 2001. Outer membrane targeting of passenger proteins by the vacuolating cytotoxin autotransporter of *Helicobacter pylori*. *Infect. Immun.* 69:6769–6775.
 20. Schmitt W, Haas R. 1994. Genetic analysis of the *Helicobacter pylori* vacuolating cytotoxin: structural similarities with the IgA protease type of exported protein. *Mol. Microbiol.* 12:307–319.
 21. Telford JL, Ghiara P, Dell'Orco M, Comanducci M, Burrone D, Bugnoli M, Tecce MF, Censini S, Covacci A, Xiang Z, et al. 1994. Gene structure of the *Helicobacter pylori* cytotoxin and evidence of its key role in gastric disease. *J. Exp. Med.* 179:1653–1658.
 22. Dautin N, Bernstein HD. 2007. Protein secretion in gram-negative bacteria via the autotransporter pathway. *Annu. Rev. Microbiol.* 61:89–112.
 23. Henderson IR, Navarro-Garcia F, Desvaux M, Fernandez RC, Ala'Aldeen D. 2004. Type V protein secretion pathway: the autotransporter story. *Microbiol. Mol. Biol. Rev.* 68:692–744.
 24. Leyton DL, Rossiter AE, Henderson IR. 2012. From self sufficiency to dependence: mechanisms and factors important for autotransporter biogenesis. *Nat. Rev. Microbiol.* 10:213–225.
 25. Gangwer KA, Mushrush DJ, Stauff DL, Spiller B, McClain MS, Cover TL, Lacy DB. 2007. Crystal structure of the *Helicobacter pylori* vacuolating toxin p55 domain. *Proc. Natl. Acad. Sci. U. S. A.* 104:16293–16298.
 26. Junker M, Schuster CC, McDonnell AV, Sorg KA, Finn MC, Berger B, Clark PL. 2006. Pertactin beta-helix folding mechanism suggests common themes for the secretion and folding of autotransporter proteins. *Proc. Natl. Acad. Sci. U. S. A.* 103:4918–4923.
 27. Renn JP, Clark PL. 2008. A conserved stable core structure in the passenger domain beta-helix of autotransporter virulence proteins. *Biopolymers* 89:420–427.
 28. Olofsson A, Vallström A, Petzold K, Tegtmeyer N, Schleucher J, Carlsson S, Haas R, Backert S, Wai SN, Gröbner G, Arnqvist A. 2010. Biochemical and functional characterization of *Helicobacter pylori* vesicles. *Mol. Microbiol.* 77:1539–1555.
 29. Salama NR, Otto G, Tompkins L, Falkow S. 2001. Vacuolating cytotoxin of *Helicobacter pylori* plays a role during colonization in a mouse model of infection. *Infect. Immun.* 69:730–736.
 30. Lertsethtakarn P, Ottemann KM, Hendrixson DR. 2011. Motility and chemotaxis in *campylobacter* and *Helicobacter*. *Annu. Rev. Microbiol.* 65:389–410.
 31. O'Toole PW, Lane MC, Porwollik S. 2000. *Helicobacter pylori* motility. *Microbes Infect.* 2:1207–1214.
 32. Kostrzynska M, Betts JD, Austin JW, Trust TJ. 1991. Identification, characterization, and spatial localization of two flagellin species in *Helicobacter pylori* flagella. *J. Bacteriol.* 173:937–946.
 33. Schirm M, Soo EC, Aubry AJ, Austin J, Thibault P, Logan SM. 2003. Structural, genetic and functional characterization of the flagellin glycosylation process in *Helicobacter pylori*. *Mol. Microbiol.* 48:1579–1592.
 34. Suerbaum S, Josenhans C, Labigne A. 1993. Cloning and genetic characterization of the *Helicobacter pylori* and *Helicobacter mustelae* flaB flagellin genes and construction of *H. pylori* flaA- and flaB-negative mutants by electroporation-mediated allelic exchange. *J. Bacteriol.* 175:3278–3288.
 35. Eaton KA, Morgan DR, Krakowka S. 1992. Motility as a factor in the colonisation of gnotobiotic piglets by *Helicobacter pylori*. *J. Med. Microbiol.* 37:123–127.
 36. Ottemann KM, Lowenthal AC. 2002. *Helicobacter pylori* uses motility for initial colonization and to attain robust infection. *Infect. Immun.* 70:1984–1990.
 37. Jones AC, Logan RP, Foyne S, Cockayne A, Wren BW, Penn CW. 1997. A flagellar sheath protein of *Helicobacter pylori* is identical to HpaA, a putative N-acetylneuraminylactose-binding hemagglutinin, but is not an adhesin for AGS cells. *J. Bacteriol.* 179:5643–5647.
 38. Luke CJ, Penn CW. 1995. Identification of a 29 kDa flagellator sheath protein in *Helicobacter pylori* using a murine monoclonal antibody. *Microbiology* 141:597–604.
 39. Lundström AM, Blom K, Sundaeus V, Bölin I. 2001. HpaA shows variable surface localization but the gene expression is similar in different *Helicobacter pylori* strains. *Microb. Pathog.* 31:243–253.
 40. González-Rivera C, Algood HM, Radin JN, McClain MS, Cover TL. 2012. The intermediate region of *Helicobacter pylori* VacA is a determinant of toxin potency in a Jurkat T cell assay. *Infect. Immun.* 80:2578–2588.
 41. Jiménez-Soto LF, Rohrer S, Jain U, Ertl C, Sewald X, Haas R. 2012. Effects of cholesterol on *Helicobacter pylori* growth and virulence properties in vitro. *Helicobacter* 17:133–139.
 42. Loh JT, Shaffer CL, Piauzelo MB, Bravo LE, McClain MS, Correa P, Cover TL. 2011. Analysis of cagA in *Helicobacter pylori* strains from Colombian populations with contrasting gastric cancer risk reveals a biomarker for disease severity. *Cancer Epidemiol. Biomarkers Prev.* 20:2237–2249.
 43. Shaffer CL, Gaddy JA, Loh JT, Johnson EM, Hill S, Hennig EE, McClain MS, McDonald WH, Cover TL. 2011. *Helicobacter pylori* exploits a unique repertoire of type IV secretion system components for pilus assembly at the bacteria-host cell interface. *PLoS Pathog.* 7:e1002237. <http://dx.doi.org/10.1371/journal.ppat.1002237>.
 44. Ivie SE, McClain MS, Algood HM, Lacy DB, Cover TL. 2010. Analysis of a beta-helical region in the p55 domain of *Helicobacter pylori* vacuolating toxin. *BMC Microbiol.* 10:60.
 45. Croxen MA, Sisson G, Melano R, Hoffman PS. 2006. The *Helicobacter pylori* chemotaxis receptor TlpB (HP0103) is required for pH taxis and for colonization of the gastric mucosa. *J. Bacteriol.* 188:2656–2665.
 46. Aizawa SI, Dean GE, Jones CJ, Macnab RM, Yamaguchi S. 1985. Purification and characterization of the flagellar hook-basal body complex of *Salmonella typhimurium*. *J. Bacteriol.* 161:836–849.
 47. Akiba T, Yoshimura H, Namba K. 1991. Monolayer crystallization of flagellar L-P rings by sequential addition and depletion of lipid. *Science* 252:1544–1546.
 48. Schuster SC, Bauerelein E. 1992. Location of the basal disk and a ringlike cytoplasmic structure, two additional structures of the flagellar apparatus of *Wolfinella succinogenes*. *J. Bacteriol.* 174:263–268.
 49. Algood HM, Allen SS, Washington MK, Peek RM, Jr, Miller GG, Cover TL. 2009. Regulation of gastric B cell recruitment is dependent on IL-17 receptor A signaling in a model of chronic bacterial infection. *J. Immunol.* 183:5837–5846.